



This work is licensed under a Creative Commons Attribution-NonCommercial 4.0 International License.

# Diffusion-Weighted Magnetic Resonance Imaging Value in the Detection and Differentiation of Bone Tumors and Tumor-Like Lesions

Mostafa M. Emara<sup>1</sup>, Ayman Nada<sup>1</sup>, Maged A. Hawana<sup>2</sup>, Mohamed S. Elazab<sup>1</sup>, Ahmed Mohamed Shokry<sup>1</sup>

## ABSTRACT

**Objective:** The aim of this study was to evaluate the ability of diffusion-weighted magnetic resonance imaging (MRI) and its corresponding apparent diffusion coefficient (ADC) values in the detection, characterization, and discrimination between different types of bony lesions.

**Materials and Methods:** Patients were evaluated by conventional and diffusion-weighted MR images. Diffusion was carried out using the b values of 0, 500, and 1000, and then the ADCs were generated.

**Results:** The average ADC value of benign lesions was approximately  $1.84 \times 10^{-3} \text{ mm}^2/\text{s} \pm 0.33$ , while that of malignant lesions was approximately  $1.17 \times 10^{-3} \text{ mm}^2/\text{s} \pm 0.44$ ;  $p < 0.001$ . The receiver operating characteristic (ROC) curve analysis produced a cut-off value for the detection of malignancy of  $1.47 \times 10^{-3} \text{ mm}^2/\text{s}$  with 89.5% specificity and 79.5% sensitivity.

**Conclusion:** Diffusion-weighted imaging combined with ADC values is considered a useful tool that can be added to the conventional MRI sequences for detection, differentiation, and characterization of different bony lesions.

**Keywords:** Magnetic resonance imaging (MRI), diffusion-weighted imaging (DWI), apparent diffusion coefficient (ADC), bone tumors, benign, malignant, tumor like

**Cite this article as:**  
Emara MM, Nada A, Hawana MA, Elazab MS, Shokry AM. Diffusion-Weighted Magnetic Resonance Imaging Value in the Detection and Differentiation of Bone Tumors and Tumor-Like Lesions Erciyas Med J 2019; 41(2): 141-7.

<sup>1</sup>Department of Diagnostic and Interventional Radiology, National Cancer Institute, Cairo University, Cairo, Egypt  
<sup>2</sup>Department of Diagnostic and Interventional Radiology, Cairo University Kasr Al Ainy Faculty of Medicine, Cairo, Egypt

Submitted  
06.01.2019

Accepted  
21.03.2019

Available Online Date  
17.05.2019

**Correspondence**  
Ayman Nada,  
Neuroradiology Fellow  
Radiology Department  
University of Missouri  
One Hospital Dr, Columbia,  
MO, 65212, USA  
Phone: 3125437524  
e.mail:  
anvr@health.missouri.edu

©Copyright 2019 by Erciyas  
University Faculty of Medicine -  
Available online at  
www.erciyesmedj.com

## INTRODUCTION

Evaluation of bone tumors represents a challenge for the clinician, and radiological evaluation is critical as it helps to distinguish malignant from benign lesions. It also guides the management plan: therapy or observation of the patient. Therefore, the goal is to be able to make a distinction between benign from the malignant osseous lesions (1).

Conventional radiographs still provide important information regarding the location, definition, margin, matrix mineralization, cortical involvement, and associated periosteal reaction of the various bony lesions. Magnetic resonance imaging (MRI) is considered to be the best modality for the local extent, staging, and assessment of both the intra- and extra-compartmental extent of the bone owing to its excellent contrast resolution, tissue characterization, and multiplanar capabilities (2).

Conventional MRI plays valuable roles in the detection and evaluation of the relationship between structures near the bone tumor (3).

Most bone tumors have classic radiographic appearance, and they can be diagnosed and correlated with patient's age and clinical data. MRI can detect a non-mineralized tumor tissue and is mostly useful in the staging and assessing of therapeutic responses of bone tumors (4).

However, few benign and malignant bone tumors show atypical features and need no further investigations. One of the common diagnostic problems encountered in daily practice is finding non-malignant lesions in known patients with primary malignancies (4).

A different tissue contrast obtained using diffusion-weighted imaging (DWI) makes it a valuable tool in the identification of benign and malignant lesions. DWI has been applied in the evaluation of certain musculoskeletal tumors and has been reported to be a useful diagnostic aid (5).

Apparent diffusion coefficient (ADC) values can provide quantitative information about water molecules diffusibility in tissues, which can add value to conventional MRI (6).

High ADC measurements indicate an increase in the motion of extracellular water, as well as the cell membrane integrity loss, while low ADC values indicate decreased extracellular water or high cellularity (7).

Reports about the diagnostic value of DWI in bone tumors are limited. Most of them are focused on spine. Most

DWI applications in the bone marrow were about the differentiation between the types of compression fractures of the vertebral column.

ADC values can be indicative of benign and malignant lesions, but an overlap between their values has been reported in different studies (4, 5, 7).

The aim of this prospective study is to evaluate the potential application of diffusion-weighted MRI in the detection, differentiation, and characterization of bone tumor entities and to correlate the diffusion patterns and ADC values of different lesions with their pathological nature.

## MATERIALS and METHODS

### Patient Selection and Clinical Assessment

This prospective study took place from December 2014 to January 2017 after an ethical approval was obtained in October 2014 from the ethic committee of the faculty of medicine (Cairo University), permit number 534/014.

Patients with clinical findings suggestive of bony lesions such as bony pain, swelling, and limitation of movement were selected.

Patients were categorized into three groups:

- (I) Benign bone tumors
- (II) Malignant bone tumors
- (III) Tumor-like lesions

All cases with MRI contraindications, such as a peace maker or metallic prosthesis causing marked artifacts, were excluded from the study.

### MRI Imaging Protocol

Imaging was done with a 1.5T superconducting MR machine (Achieva XR, MRI Philips, Netherlands), using the most optimal surface coil to accommodate each lesion, that is, either a body coil or phase-arrayed torso coil (16 channels).

The MRI protocol included the conventional T1, T2, STIR, and DWI, as well as post-contrast fat-suppressed T1-weighted images.

Post-contrast assessment: After intravenous administration of gadolinium DPTA in a dose of 0.1 mmol/kg, multiplanar T1 fat suppression was obtained immediately.

Diffusion-weighted MRI: Images were obtained using a multi-section single-shot spin echo-planar sequence with diffusion sensitivities of b values equal to 0, 500, and 1000 s/mm<sup>2</sup>.

Three different b values were chosen to obtain more accurate data about the diffusion map, b<sub>0</sub> considered the base of the diffusion map, and the higher the value used, the more sensitive data were given. For example, cystic lesion shows a drop of their diffusion high signal at higher b values.

Diffusion gradients were applied sequentially in three orthogonal directions (X, Y, and Z), using sections 5 mm in thickness, with an interslice gap of 1 mm, the field of view 240–400 mm, 128x256 matrix, and the scanning time of approximately 120 s for all images.

Post-processing of DWI: Four sets of DWIs for each section were

obtained. The first three sets of images (trace images) were corresponding to the sequential application of the sensitization gradient in the X, Y, and Z planes. The last set is the ADC maps.

### Quantitative Image Analysis

1. The lesion was determined on the DWI and ADC map using the conventional MR images as a guide.
2. The signal intensity of the lesion on DWIs (b1000) was determined: either hypointense equals free diffusion, or hyperintense equals restricted diffusion.
3. Measurements of the ADC were made using an electronic cursor on the ADC map in different regions of interest (ROI) of the lesions and in comparable contralateral regions of the normal tissue. The ADC values were expressed in 10<sup>-3</sup> mm<sup>2</sup>/s.
4. ROI was calculated based on 1 cm placed at 3 different sites, then the average was calculated.
5. ROI was placed at the most restricted areas of the solid part guided by the conventional images, the areas of the most appreciable signal changes and post-contrast enhancement, are placed within the center of the cystic component. ROI for the areas which were too small, hemorrhagic, or adjacent to the vessels was excluded to avoid misinterpretation from the surrounding tissue in case of lesions that were too small and blood-blooming effect in hemorrhage, as well as the pulsation effect of the vessels.
6. The quality of diffusion-weighted images and ADC maps was evaluated, with the exclusion of non-acceptable images that contained distortion or the ghosting artifact.
7. Two MSK radiologists with 10 years of experience in MRI have blindly reviewed the MRI findings and the ROIs carefully chosen on ADC maps. ADC values were independently measured. Interpretation results were agreed by consent.

### Pathological Assessment

Correlation between the radiological data and pathological results of the surgically excised or biopsied lesions was done.

### Statistical Analysis

For comparison between the mean ADC values of malignant, benign, and tumor-like lesions.

### Statistical Methods

Encoded data were entered using the statistical package SPSS version 23 and found to follow the Gaussian distribution; they were then summarized to obtain the mean and standard deviation for quantitative variables and frequencies (number of cases) and relative frequencies (percentages) for categorical variables. Afterwards, comparisons were made between groups using an unpaired t-test.

The ROC curve was constructed with the area under curve analysis, which was performed to detect the best cut-off value of ADC for the detection of malignancy. A p-value of <0.05 was considered to be statistically significant.

## RESULTS

A total of 62 patients were involved in the study (34 males and 28

females) aged 1–77 years, and the mean age was 25.39. The lesions were classified as chondrogenic (Fig. 1) and non-chon-

drogenic (Fig. 2) with the non-chondrogenic representing approximately 86% of the lesions.

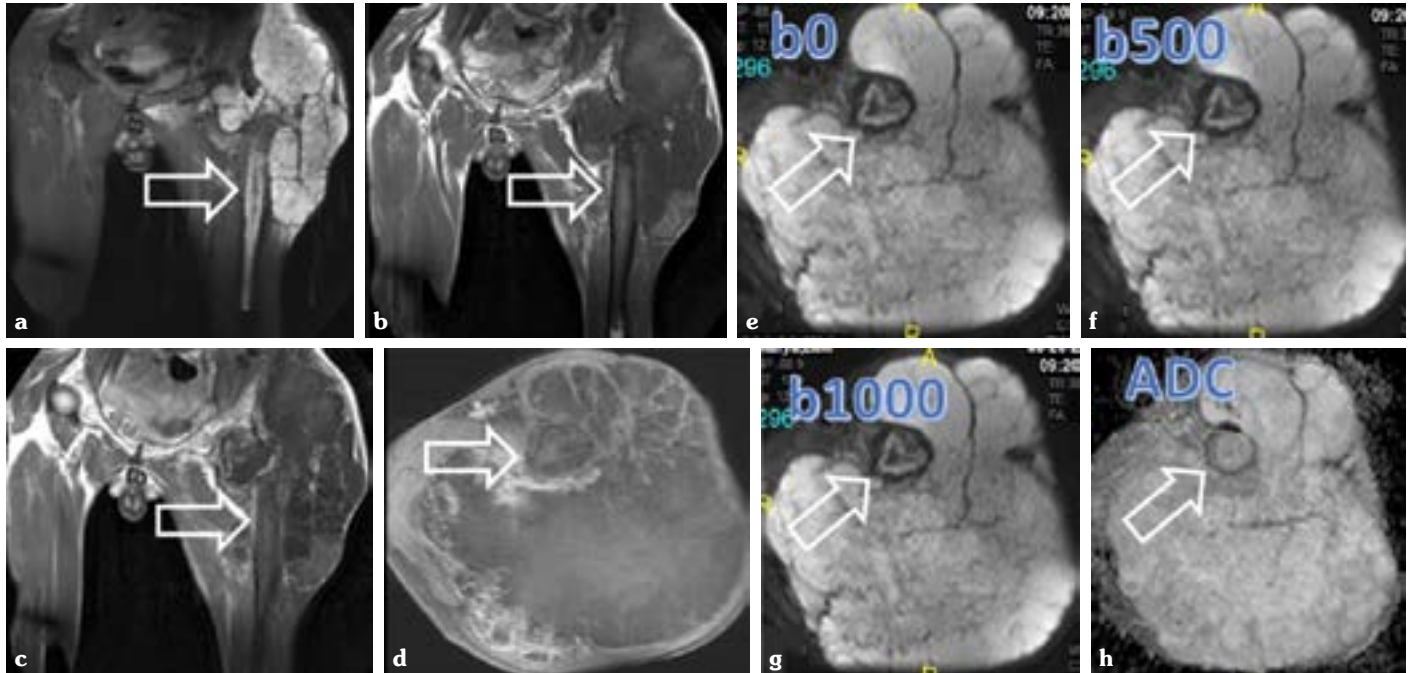


**Figure 1. a–h.** A 52-year-old male presenting with left upper-thigh and gluteal large swelling. Conventional MRI (a) coronal STIR, (b) coronal T1 WI, (c) coronal T1 post-contrast, and (d) axial T1 fat-sat post-contrast showed a left femoral and hemi-pelvic diffuse marrow infiltration of low T1 and a high STIR signal associated with a huge infiltrating soft tissue mass lesion showing an internal breaking down and hemorrhage with heterogeneous post-contrast enhancement. Diffusion-weighted MRI (e–g) b1000 and (h) ADC map demonstrated a bright signal in different b values with the mean ADC value of  $2.05 \times 10^{-3} \text{ mm}^2/\text{s}$ . A histopathological evaluation confirmed chondrosarcoma

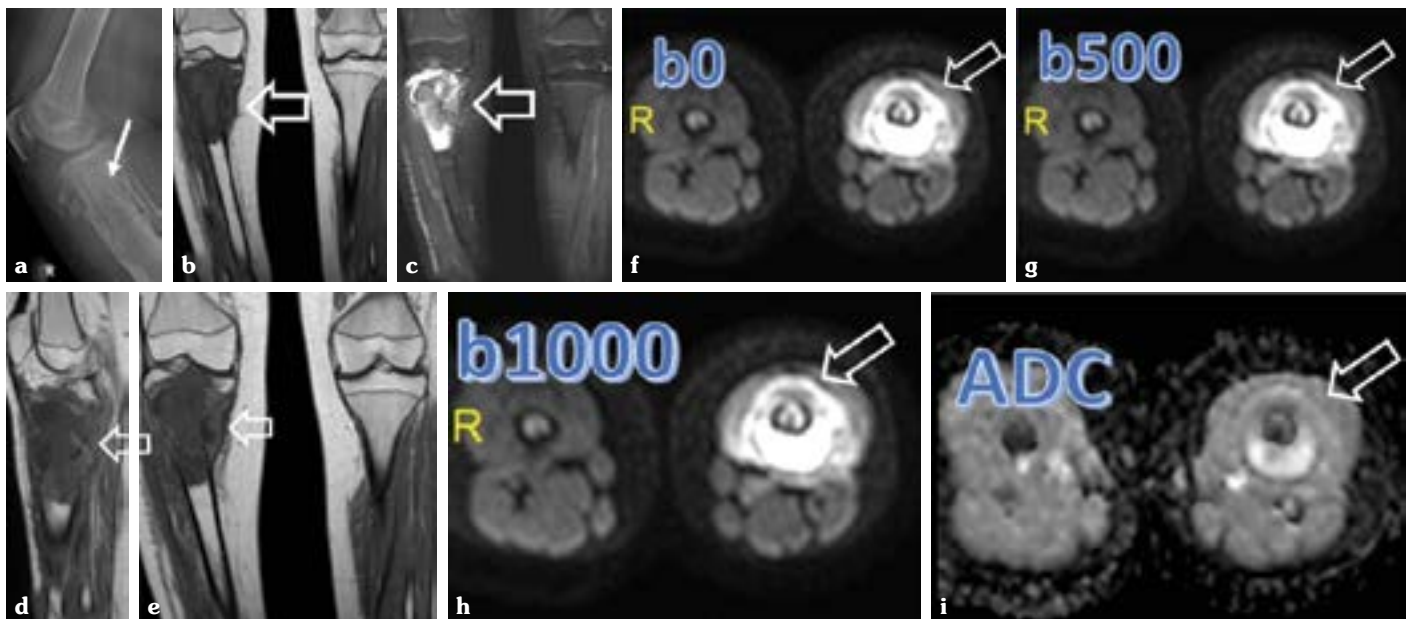


**Figure 2. a–i.** A 15-year-old male presented with right upper leg pain and swelling. Conventional digital X-RAY (a) and MRI (b) coronal T1 WI, (c) coronal STIR, (d) Sagittal T1 post contrast, and (e) coronal T1 post-contrast showed a right upper tibial shaft infiltrative marrow lesion of a low T1 and bright T2/STIR signal with heterogeneous post-contrast enhancement extending to the articular surface. Associated periosteal reaction, cortical disruption, and extra-osseous soft tissue component are noted. A lucent tunnel can be noticed in the plain x-ray representing the site of biopsy. Diffusion-weighted MRI (f–h) b1000 and (i) ADC map also demonstrated a bright signal in different b values with a low signal on the ADC map (restricted diffusion) with the mean ADC value of  $1.39 \times 10^{-3} \text{ mm}^2/\text{s}$ . A histopathological analysis revealed osteosarcoma

**Table 1.** Number and percentage of each pathology

Pathology details	n	%
Simple bone cyst	2	3.2
Recurrent ameloblastoma	1	1.6
Osteosarcoma	6	9.7
Osteoid osteoma	1	1.6
Osteochondroma	3	4.8
Multiple myeloma	4	6.5
Metastases	4	6.5
Marrow edema	2	3.2
Lymphoma	4	6.5
Lipoma	1	1.6
Langerhans cell histiocytosis	1	1.6
Inflammatory	4	6.5
Hemangioma	2	3.2
Fibrous dysplasia	1	1.6
Fibrous cortical defect	2	3.2
Ewing sarcoma	16	25.8
Enchondroma	2	3.2
Chondrosarcoma	3	4.8
Chondromyxoid fibroma	1	1.6
Aneurysmal bone cyst	2	3.2

Pathological evaluation revealed 12 (14.5%) benign lesions, 11 (17.7%) tumor-like lesions, and 39 (62.9%) malignant lesions. The radiological and pathological criteria are demonstrated in Tables 1–4.

Our study showed that the mean ADC value of benign tumors was  $1.84 \times 10^{-3} \text{ mm}^2/\text{s}$  and for malignant tumors  $1.17 \times 10^{-3} \text{ mm}^2/\text{s}$ , as well as  $1.54 \times 10^{-3} \text{ mm}^2/\text{s}$  for tumor-like lesions.

A p-value of <0.001 with a cut-off value to determine benignity vs. malignancy of 1.47 has an 89.5% specificity and 79.5% sensitivity after the ROC curve analysis with an area under the curve 0.868 (Fig. 3).

The DWI associated with the calculation of ADC values can help to distinguish

- Malignant and benign bone tumors with a significant statistical difference ( $p < 0.001$ ) and after the exclusion of chondrogenic tumors ( $p < 0.004$ ). Malignant bony tumors usually have average ADC values usually lower than  $1.47 \times 10^{-3} \text{ mm}^2/\text{s}$ , while benign bony tumors have average ADC values of approximately  $1.84 \times 10^{-3} \text{ mm}^2/\text{s}$ .
- Inflammatory and malignant bony lesions, as the average ADC values for inflammatory lesions are usually greater than  $1.61 \times 10^{-3} \text{ mm}^2/\text{s}$ . For example, Ewing sarcoma always has a mean ADC value of approximately  $0.74 \times 10^{-3} \text{ mm}^2/\text{s}$ , so it can be distinguished from osteomyelitis.
- Solid and cystic lesions (without the need of contrast media) as cystic lesions always have an average ADC value higher than  $2.13 \times 10^{-3} \text{ mm}^2/\text{s}$ .

**Table 2.** Detailed diffusion character for each pathology

Pathology details	Non-restricted		Restricted	
	Count	Column n %	Count	Column n %
SBC	2	7.1%	0	.0%
Recurrent ameloblastoma	0	.0%	1	2.9%
Osteosarcoma	1	3.6%	5	14.7%
Osteoid osteoma	1	3.6%	0	.0%
Osteochondroma	3	10.7%	0	.0%
Multiple myeloma	1	3.6%	3	8.8%
Metastases	1	3.6%	3	8.8%
Marrow edema	2	7.1%	0	.0%
Lymphoma	1	3.6%	3	8.8%
Lipoma	1	3.6%	0	.0%
Langerhans cell histiocytosis LCH	0	.0%	1	2.9%
Inflammatory	3	10.7%	1	2.9%
Hemangioma	2	7.1%	0	.0%
Fibrous dysplasia	1	3.6%	0	.0%
Fibrous cortical defect	2	7.1%	0	.0%
Ewing sarcoma	0	.0%	16	47.1%
Enchondroma	2	7.1%	0	.0%
Chondrosarcoma	2	7.1%	1	2.9%
Chondromyxoid fibroma	1	3.6%	0	.0%
Aneurysmal bone cyst ABC	2	7.1%	0	.0%

SBC: Simple bone cyst; LCH: Langerhans cell histiocytosis; ABC: Aneurysmal bone cyst

- Mild statistical difference between tumor-like and benign bony lesions ( $p < 0.041$ ), while significant statistical difference between tumor-like and malignant bony lesions was detected ( $p < 0.007$ ).

## DISCUSSION

Tissue characterization using conventional MRI can be improved by adding the value of DWI. Although some lesions show specific diagnostic imaging features, surgical biopsy is still the only way to make an accurate diagnosis.

Our aim in this study was to direct the invasive diagnostic measures and decrease the percentage of unnecessary biopsies of benign lesions, as well as to aid the follow-up of tumors. In our study, tumors were assessed qualitatively and quantitatively by measuring the ADC values.

Due to their high contrast-to-noise ratio, lesions showing restricted diffusion can be usually recognized on DWI (8), but without any clear anatomical details. This is explained by a decreased spatial resolution of the DWIs in comparison to conventional MR images as stated by Vermoolen et al. (2012) (9).

Park et al. (2007) (10) argued that DWIs and ADC may not be able to distinguish small lesions and that those have a similar grade of diffusivity. Neubauer et al. (2012) (11) supposed that false low

**Table 3.** Mean ADC value for each pathology

	ADC values for solid component		ADC values for cystic component	
	Mean	SD	Mean	SD
SBC	-	-	2.55	.07
Recurrent ameloblast	1.50	-	-	-
Osteosarcoma	1.38	.03	-	-
Osteoid osteoma	1.36	-	-	-
Osteochondroma	2.18	.01	-	-
Multiple myeloma	1.41	.02	-	-
Metastases	1.25	.06	-	-
Marrow edema	1.67	.04	-	-
Lymphoma	1.60	.08	-	-
Lipoma	1.50	-	-	-
LCH	1.10	-	-	-
Inflammatory	1.61	.06	2.13	.02
Hemangioma	1.60	.00	-	-
Fibrous dysplasia	1.00	-	-	-
Fibrous cortical defect	1.56	.02	-	-
Ewing sarcoma	.74	.19	-	-
Enchondroma	2.12	.01	-	-
Chondrosarcoma	2.03	.03	-	-
Chondromyxoid fibroma	2.10	-	-	-
ABC	-	-	2.45	.07

ADC; Apparent diffusion coefficient; SD: Standard deviation; SBC: Simple bone cyst; LCH: Langerhans cell histiocytosis; ABC: Aneurysmal bone cyst

ADC measurements of small-target lesions can be due to partial volume effects. Recommendations by Padhani et al. (2009) (12) suggest a cut-off value not less than 1 cm in the lesion diameter. This was applied in our study where sub-centimetric lesions were identified but were omitted from the study due to a small ROI, which would have not given valuable results.

A disadvantage of the visual DWI assessment is that an area with a very long T2 relaxation time will have a persistent high signal and may interpreted falsely as restricted diffusion (9). In our study, all the benign cystic lesions showed an elevated signal intensity that sometimes persisted even with elevated b values (b1000) due to the

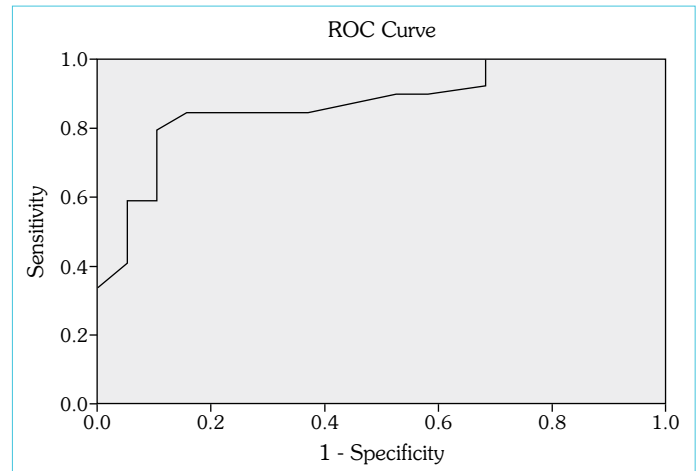


**Figure 3.** ROC curve for the detection of malignancy using ADC values

“T2 shine through” effect simulating more aggressive tumors with true restriction. This false impression was corrected by the correlation of each lesion with the ADC map for an accurate judgment of the lesions.

The ADC measurement differentiates tissues according to their water content and their diffusivity by applying high maximum b values (10). In our study b1000 lead to an adequate background suppression and dampening of the signal given by cystic areas of necrosis in malignant lesions and fluid in benign lesions. This is also supported by Tang et al. (2007) (13).

Chondroid tumors have a fluid-rich matrix, so there is no appreciated difference between the ADC measurements in benign and malignant lesions (Hayashida et al., 2006) (14). We also agree that there is no appreciated ADC difference between the benign and malignant chondroid tumors as the mean ADC value for benign chondroid tumors was  $2.14 \times 10^{-3} \text{ mm}^2$ , while for malignant chondroid tumors, it was  $2.03 \times 10^{-3} \text{ mm}^2$ .

Two cases of vertebral bodies hemangiomas were present showing an ADC value of approximately  $1.6 \times 10^{-3} \text{ mm}^2$ . This is in agreement with Kotb et al. (2014) (15).

Inflammatory lesions considered to be common tumor-like lesions (36.3%) were showing relatively high ADC values of approximately  $1.61 \times 10^{-3} \text{ mm}^2$  (Fig. 4), so the discrimination between them and Ewing sarcoma found to have the mean ADC value of approximately  $0.74 \times 10^{-3} \text{ mm}^2$  can be done clearly, in agreement with

**Table 4.** Mean ADC values for benign and malignant chondrogenic and non-chondrogenic lesions

		Pathology					
		Chondrogenic			Non-chondrogenic		
		Benign	Tumor like	Malignant	Benign	Tumor like	Malignant
ADC values for solid component	Mean	2.14	-	2.03	1.53	1.54	1.10
	SD	.04	-	.03	.09	.25	.37

ADC: Apparent diffusion coefficient; SD: Standard deviation



**Figure 4. a–j.** A 6-year-old female presenting with left lower-thigh pain and swelling with a limited movement. Conventional digital X-RAY (a) and MRI (b) axial T1 WI, (c) axial T2 WI, (d) axial T1 fat sat post-contrast, (e) sagittal T1 post-contrast, and (f) coronal T1 post-contrast showed a metadiaphyseal diffuse altered marrow signal displaying heterogeneous a low T1 and bright T2/STIR signal associated with periosteal reaction, muscular edema, and extra-osseous posteriorly located marginally enhancing fluid collection. Diffusion-weighted MRI (g–i) b1000 and (j) ADC maps demonstrated a bright signal in different b values with the mean ADC value of  $2.15 \times 10^{-3} \text{ mm}^2/\text{s}$  for the cystic component and  $1.6 \times 10^{-3} \text{ mm}^2/\text{s}$  for the solid component. A histopathological analysis revealed an osteomyelitis inflammatory process

Andrew et al. (2018) (16). The abscesses of an osteomyelitis sequel have contents with elevated viscosity, so it shows restricted diffusion and a low ADC value in agreement with Wong et al. (2004) (17).

The ADC values of solid malignant tumors (n=39) ranged from  $0.74$  to  $2.03 \times 10^{-3} \text{ mm}^2$  with the mean ADC  $1.17 \times 10^{-3} \text{ mm}^2$ . This big variation was explained by differences in tumor cellularity, extracellular stromal density, and tortuosity in agreement with Humphries et al. (2007) (18).

We also agree with Nagata et al. (2005) (19) and Oh et al. (2017) (20), who recommended exclusion of cartilaginous tumors from other malignant tumors due to their markedly high ADC value, so after the exclusion of chondrosarcoma, malignant tumors will range from  $0.6$  to  $1.6 \times 10^{-3} \text{ mm}^2$  with the mean ADC  $1.1 \times 10^{-3} \text{ mm}^2$ . Ewing sarcoma and undifferentiated carcinoma had the most decreased ADC value among the malignant tumors.

The limitations of our study were the lack of benign and tumor-like lesions in comparison to malignant lesions, and a low number of some of bone pathologies, like chondrogenic tumors, for which diagnosis plain X-ray may sometimes be enough without the need for routine MRI.

## CONCLUSION

Clinically, skeletal lesions in children and adults range from benign to aggressive malignancy, so the need for a non-invasive helpful diagnostic tool was necessary.

DWI can be a valuable tool to make a distinction between different bony lesions when used side by side with conventional MRI after the calculation of ADC values.

**Ethics Committee Approval:** This prospective study took place from December 2014 to January 2017 after an ethical approval was obtained in October 2014 from the ethic committee of the faculty of medicine (Cairo University), permit number 534/014.

**Informed Consent:** Written informed consent was obtained from patients who participated in this study.

**Peer-review:** Externally peer-reviewed.

**Author Contributions:** Designed the study: EM. Collected the data: EM. Analyzed the data: ME, MH. Wrote the paper: NA. Revised the manuscript: SA. All authors have read and approved the final manuscript.

**Conflict of Interest:** The authors have no conflict of interest to declare.

**Financial Disclosure:** The authors declared that this study has received no financial support.

## REFERENCES

1. Baweja S, Arora R, Singh S, Sharma A, Narang P, Ghuman S, et al. Evaluation of bone tumors with magnetic resonance imaging and correlation with surgical and gross pathological findings. *Indian J Radiol Imaging* 2006; 16: 611–8. [CrossRef]
2. Nomikos GC, Murphey MD, Kransdorf MJ, Bancroft LW, Peterson JJ. Primary bone tumors of the lower extremities. *Radiol Clin North Am* 2002; 40(5): 971–90. [CrossRef]
3. Subhawong TK, Jacobs MA, Fayad LM. Diffusion-weighted MR imaging for characterizing musculoskeletal lesions. *Radiographics* 2014; 34(5): 1163–77. [CrossRef]
4. Pekcevik Y, Kahya MO, Kaya A. Diffusion-weighted Magnetic Resonance Imaging in the Diagnosis of Bone Tumors: Preliminary Results. *J Clin Imaging Sci* 2013; 3: 63. [CrossRef]
5. Yakushiji T, Oka K, Sato H, Yorimitsu S, Fujimoto T, Yamashita Y, et al. Characterization of chondroblastic osteosarcoma: gadolinium-enhanced versus diffusion-weighted MR imaging. *J Magn Reson Imaging* 2009; 29(4): 895–900. [CrossRef]
6. Bley TA, Wieben O, Uhl M. Diffusion-weighted MR imaging in musculoskeletal radiology: applications in trauma, tumors, and inflammation. *Magn Reson Imaging Clin N Am* 2009; 17(2): 263–75. [CrossRef]
7. Taskin G, Incesu L, Aslan K. The value of apparent diffusion coefficient measurements in the differential diagnosis of vertebral bone marrow lesions. *Turk J Med Sci* 2013; 43(3): 379–87. [CrossRef]
8. Biffar A, Dietrich O, Sourbron S, Duerr HR, Reiser MF, Baur-Melnyk A. Diffusion and perfusion imaging of bone marrow. *Eur J Radiol* 2010; 76(3): 323–8. [CrossRef]
9. Vermoolen MA, Kwee TC, Nieuwenstein RA. Apparent diffusion coefficient

- cient measurements in the differentiation between benign and malignant lesions: a systematic review. *Insights Imaging* 2012; 3(4): 395–409.
10. Park MJ, Cha ES, Kang BJ, Ihn YK, Baik JH. The role of diffusion-weighted imaging and the apparent diffusion coefficient (ADC) values for breast tumors. *Korean J Radiol* 2007; 8(5): 390–6. [\[CrossRef\]](#)
  11. Neubauer H, Evangelista L, Hassold N, Winkler B, Schlegel PG, Köstler H, et al. Diffusion-weighted MRI for detection and differentiation of musculoskeletal tumorous and tumor-like lesions in pediatric patients. *World J Pediatr* 2012; 8(4): 342–9. [\[CrossRef\]](#)
  12. Padhani AR, Liu G, Koh DM, Chenevert TL, Thoeny HC, Takahara T, et al. Diffusion-weighted magnetic resonance imaging as a cancer-biomarker: consensus and recommendations. *Neoplasia* 2009; 11(2): 102–25. [\[CrossRef\]](#)
  13. Tang G, Liu Y, Li W, Yao J, Li B, Li P. Optimization of b value in diffusion-weighted MRI for the differential diagnosis of benign and malignant vertebral fractures. *Skeletal Radiol* 2007; 36(11): 1035–41.
  14. Hayashida Y, Yakushiji T, Awai K, Katahira K, Nakayama Y, Shimomura O, et al. Monitoring therapeutic responses of primary bone tumors by diffusion-weighted image: Initial results. *Eur Radiol* 2006; 16(12): 2637–43. [\[CrossRef\]](#)
  15. Kotb SZ, Sultan AA, Elhawary GM, Taman SE. Value of diffusion weighted MRI in differentiating benign from malignant bony tumors and tumor like lesions. *The Egyptian Journal of Radiology and Nuclear Medicine* 2014; 45(2): 467–76. [\[CrossRef\]](#)
  16. Degnan AJ, Chung CY, Shah AJ. Quantitative diffusion-weighted magnetic resonance imaging assessment of chemotherapy treatment response of pediatric osteosarcoma and Ewing sarcoma malignant bone tumors. *Clin Imaging* 2018; 47: 9–13. [\[CrossRef\]](#)
  17. Wong AM, Zimmerman RA, Simon EM, Pollock AN, Bilaniuk LT. Diffusion-weighted MR imaging of subdural empyemas in children. *AJNR Am J Neuroradiol* 2004; 25(6): 1016–21.
  18. Humphries PD, Sebire NJ, Siegel MJ, Olsen ØE. Tumors in pediatric patients at diffusion-weighted MR imaging: apparent diffusion coefficient and tumor cellularity. *Radiology* 2007; 245(3): 848–54. [\[CrossRef\]](#)
  19. Nagata S, Nishimura H, Uchida M, Hayabuchi N. [Usefulness of diffusion-weighted MRI in differentiating benign from malignant musculoskeletal tumors]. [Article in Japanese]. *Nihon Igaku Hoshasen Gakkai Zasshi* 2005; 65(1): 30–6.
  20. Oh E, Yoon YC, Kim JH, Kim K. Multiparametric approach with diffusion-weighted imaging and dynamic contrast-enhanced MRI: a comparison study for differentiating between benign and malignant bone lesions in adults. *Clin Radiol* 2017; 72(7): 552–9. [\[CrossRef\]](#)